

# Physical Simulation of Moisture Induced Thin Shell Deformation

ANONYMOUS AUTHOR(S)

## ACM Reference Format:

Anonymous Author(s). 2018. Physical Simulation of Moisture Induced Thin Shell Deformation. 1, 1 (November 2018), 4 pages. <https://doi.org/10.1145/888888.777777>

## 1 INTRODUCTION

*Contribution.* We present a low-order discrete shell model tailored to simulating non-uniform, anisotropic, differential swelling and shrinking of thin shells. In contrast to previous methods for simulating related phenomena, such as burning and growth, our formulation builds on discrete geometric shell theory and supports arbitrary rest curvature and strain, and physical settings such as thickness and Lamé parameters. We couple our shell model to a simple formulation of moisture diffusion in both the lateral and thickness directions, which takes into account anisotropy of the material grain. In a series of experiments, we show that our model successfully predicts the qualitative behavior of thin shells undergoing complex, dynamic deformations due to swelling or shrinking, such as occurs when paper is moistened, leaves dry in the sun, or thin plastic melts.

### 1.1 Related Work

in-plane growth with Loop subdivision [Vetter et al. 2013]

## 2 CONTINUOUS FORMULATION

Before describing our discretization of shells, we briefly review the formulation in the continuous setting, as this formulation will guide our discretization.

*Shell Geometry.* We can represent shells  $S \subset \mathbb{R}^3$  of thickness  $h$  by a parameter domain  $\Omega$  in the plane and an embedding  $\phi : \Omega \times [-h/2, h/2] \rightarrow \mathbb{R}^3$  with  $S$  the image of  $\phi$  (see Figure ??). We adopt the common Kirchhoff-Love assumption that the shell does not undergo any transverse shear; ie, that the shell volume is foliated by normal offsets of the shell's *midsurface*  $\mathbf{r} : \Omega \rightarrow \mathbb{R}^3$ . In other words,

$$\phi(x, y, z) = \mathbf{r}(x, y) + z\hat{\mathbf{n}}(x, y)$$

where  $\hat{\mathbf{n}} = (\mathbf{r}_x \times \mathbf{r}_y) / \| \mathbf{r}_x \times \mathbf{r}_y \|$  is the midsurface normal. The shell's deformation is thus completely determined by the deformation of the midsurface. The metric  $g$  on the slab  $\Omega \times [-h/2, h/2]$ , pulled back from  $\mathbb{R}^3$ , can be expressed in terms of the geometry of the midsurface:

$$g = \begin{bmatrix} a - 2zb + z^2c & 0 \\ 0 & 1 \end{bmatrix},$$

where

$$a = d\mathbf{r}^T d\mathbf{r} \quad b = -d\mathbf{r}^T d\hat{\mathbf{n}} \quad c = d\hat{\mathbf{n}}^T d\hat{\mathbf{n}}$$

Permission to make digital or hard copies of part or all of this work for personal or classroom use is granted without fee provided that copies are not made or distributed for profit or commercial advantage and that copies bear this notice and the full citation on the first page. Copyrights for third-party components of this work must be honored. For all other uses, contact the owner/author(s).

© 2018 Copyright held by the owner/author(s).

XXXX-XXXX/2018/11-ART

<https://doi.org/10.1145/888888.777777>

are the classical first, second, and third fundamental forms of the surface  $\mathbf{r}$ .

Oftentimes, the parameterization domain of a thin shell is assumed to be also the rest state of the shell, so that the strain in the material of the shell can be determined directly from looking at  $g$ . We cannot assume this: consider for instance a piece of paper whose center has been moistened by spilled coffee. The fibers in the coffee stain stretch; since they are confined by the surrounding non-wet region of the paper, the paper cannot globally stretch in such a way that both the wet and dry regions of the paper are simultaneously at rest. Instead, the paper will *buckle* out of plane, into a shape that compromises between relaxing the in-plane (stretching) strain and the introduced bending strain. At this point the paper's rest state is *non-Euclidean*—it is impossible to find any embedding of the paper into  $\mathbb{R}^3$  that is entirely strain-free.

We therefore record the rest state of the shell using a *rest metric*  $\bar{g}(x, y, z)$ .<sup>1</sup> Since our model is tailored to simulating differential in-plane swelling or shrinking across the thickness of the shell, we make the simplifying assumption that this rest metric is linear in the thickness direction, and does not affect the shell thickness:

$$\bar{g}(x, y, z) = \bar{a}(x, y) - 2z\bar{b}(x, y).$$

A shell that begins a simulation at rest will simply have  $\bar{a} = a$  and  $\bar{b} = b$ ; similarly, in the case that the shell *does* have a rest state  $\bar{\mathbf{r}}$  that is isometrically embeddable in  $\mathbb{R}^3$ ,  $a$  and  $b$  are the first and second fundamental forms of the surface  $\bar{\mathbf{r}}$ . Therefore  $a$  and  $b$  can be thought of as representing the “rest metric” and “rest curvature” of the shell, respectively.<sup>2</sup>

Finally, we cannot assume that the shell has uniform density, since different parts of the shell might gain or lose mass due to absorbing or releasing moisture. We therefore allow the density per unit *rest* volume  $\rho(x, y)$  to vary over  $\Omega$ . (In principle, we could also model the variation in density across the shell thickness; however doing so leads only to a small ( $O(h^3)$ ) correction to the shell's kinetic energy, and since the swelling phenomena we are interested in simulating tend to happen over relatively long time scales, there is no need for such accuracy.)

To summarize, our parameterization of thin shells involves the following kinematic elements:

- a thickness  $h$  and parameterization domain  $\Omega \subset \mathbb{R}^2$ , both of which are fixed over the course of the simulation;
- an embedding  $\mathbf{r} : \Omega \rightarrow \mathbb{R}^3$  representing the shell midsurface's “current”/“deformed” geometry, and which evolves over time. From this midsurface embedding, the embedding of the full shell volume  $\phi$ , and the midsurface fundamental forms, can be calculated;

<sup>1</sup>Here and throughout the paper, we use an overbar to denote quantities associated to the shell rest state.

<sup>2</sup>We stress, though, that these labels are to provide intuition only— $\bar{a}$  and  $\bar{b}$  must not, and generally will not, satisfy usual relationships from differential geometry such as the Gauss-Codazzi-Mainardi equations.

- 115 • a rest metric and density, parameterized by the pair of tensor  
 116 field  $\bar{\mathbf{a}}, \bar{\mathbf{b}}$  and a scalar field  $\rho$  over  $\Omega$ , respectively. These might  
 117 also evolve over time, due to changes in the shell rest state  
 118 via growth or shrinkage.

## 120 2.1 Shell Dynamics

121 Motivated by the common observation that a sufficiently thin shell  
 122 bends much more readily than it will stretch, we assume that the  
 123 shell's deformation involves *large rotations* but only small in-plane  
 124 strain of the midsurface:  $\|\bar{\mathbf{a}}^{-1}\mathbf{a} - I\|_\infty < h$ . We also assume that  
 125 the shell's material is uniform and isotropic. The simplest constitutive  
 126 law consistent with these assumptions is to use a St. Venant-  
 127 Kirchhoff material model<sup>3</sup> together with Green strain; it can be  
 128 shown [] that these choices yield an elastic energy density that can  
 129 be approximated up to  $O(h^4)$  by

$$130 W(x, y) = \left( \frac{h}{4} \|\bar{\mathbf{a}}^{-1}\mathbf{a} - I\|_{SV}^2 + \frac{h^3}{12} \|\bar{\mathbf{a}}^{-1}(\mathbf{b} - \bar{\mathbf{b}})\|_{SV}^2 \right) \sqrt{\det \bar{\mathbf{a}}}$$

133 where  $\|\cdot\|_{SV}$  is the "St. Venant-Kirchhoff norm"[]

$$134 \|M\|_{SV} = \frac{\alpha}{2} \operatorname{tr}^2 M + \beta \operatorname{tr}(M^2),$$

136 for Lamé parameters  $\alpha, \beta$ . In terms of the Young's modulus  $E$  and  
 137 Poisson's ratio  $\nu$ ,

$$138 \alpha = \frac{E\nu}{(1+\nu)(1-2\nu)}, \quad \beta = \frac{E}{2(1+\nu)}.$$

140 We thus have a formulation of kinetic energy and potential energy

$$142 T[\mathbf{r}] = \int_{\Omega} h\rho \|\dot{\mathbf{r}}\|^2 \sqrt{\det \bar{\mathbf{a}}} dx dy, \quad V[\mathbf{r}] = \int_{\Omega} W(x, y) dx dy,$$

144 to which additional external energies and forces (gravity, constraint  
 145 forces, etc) can be added to yield equations of motion via the usual  
 146 principle of least action.

## 147 3 DISCRETIZATION

## 149 4 MOISTURE DIFFUSION

## 150 5 RESULT

152 5.0.1 *Radially Wet Disc*.

153 5.0.2 *Machine Direction Experiment*.

154 5.0.3 *Dried Leaves*.

156 5.0.4 *Wetting Paper Annulus*.

158 5.0.5 *Wetting Straw Wrapping Paper*.

159 5.0.6 *Melting Spoon*.

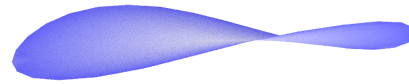
161 5.0.7 *Melting Torus*.

## 162 6 CONCLUSIONS AND FUTURE WORK

## 164 REFERENCES

165 Roman Vetter, Norbert Stoop, Thomas Jenni, Falk K. Wittel, and Hans-Joachim Hermann. 2013. Subdivision shell elements with anisotropic growth. *Internat. J. Numer. Methods Engrg.* 95, 9 (2013), 791–810. <https://doi.org/10.1002/nme.4536>

168 <sup>3</sup>The neo-Hookean material model is also popular in computer graphics and could be  
 169 used instead, although there is little benefit to doing so when simulating thin shells  
 170 since strains are typically small.

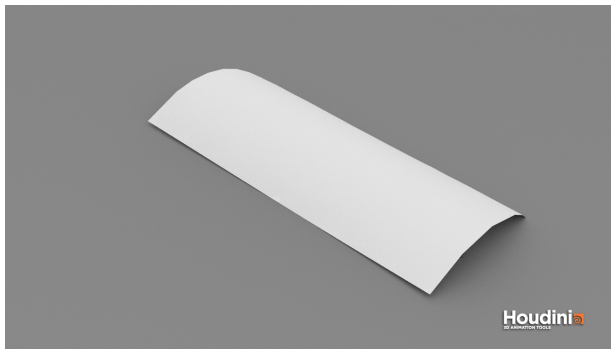


(a) Caption 1

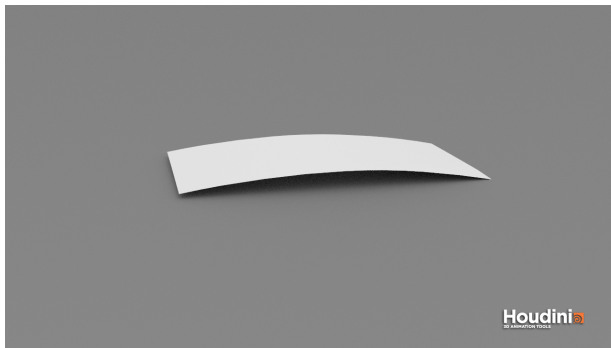


(b) Caption 2

loucini



(a) Caption1



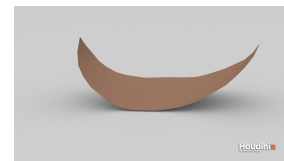
(b) Caption 2



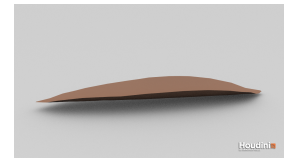
(a) Caption1



(b) Caption 2



(c) Caption1



(d) Caption 2

Fig. 3. Simulation for Dried Leaves

229  
230  
231  
232  
233  
234  
235  
236  
237  
238  
239  
240  
241  
242  
243  
244  
245  
246  
247  
248  
249  
250  
251  
252  
253  
254  
255  
256  
257  
258  
259  
260  
261  
262  
263  
264  
265  
266  
267  
268  
269  
270  
271  
272  
273  
274  
275  
276  
277  
278  
279  
280  
281  
282  
283  
284  
285

286  
287  
288  
289  
290  
291  
292  
293  
294  
295  
296  
297  
298  
299  
300  
301  
302  
303  
304  
305  
306  
307  
308  
309  
310  
311  
312  
313  
314  
315  
316  
317  
318  
319  
320  
321  
322  
323  
324  
325  
326  
327  
328  
329  
330  
331  
332  
333  
334  
335  
336  
337  
338  
339  
340  
341  
342



(a) Caption1



(b) Caption 2



(c) Caption1

Fig. 4. Simulation for Wet Annulus



(a) Caption1



(b) Caption 2



(c) Caption1

Fig. 5. Simulation for Dried Torus